The Development of a Rugged Weather-Resistant Continuous Holdup Monitor for Ductwork at Nuclear Facilities

K. C. Goetz[1,*], C. Brett Witherspoon[1], N. Prins[1], R. Hunneke[1], and P. W. Gibbs[1]

[1]Oak Ridge National Laboratory, Oak Ridge, Tennessee

[leave space for DOI, which will be inserted by ANS]

ABSTRACT

Researchers at Oak Ridge National Laboratory (ORNL) are developing a low-cost, distributed detector system for real-time, in situ monitoring of nuclear material holdup. This system will improve the accuracy of holdup measurements and decrease facility burden and risk to personnel by enabling longer count times and automated data analysis. Ductwork surveys for nuclear material holdup in nuclear facilities are typically conducted manually on a periodic basis and represent the highest level of effort for holdup monitoring. There can be hundreds of monitoring points. Often, monitoring points are difficult to access or pose safety hazards to the personnel recording the measurements. Additionally, count times are typically short (e.g., 6–10 seconds) due to the high number of monitoring points resulting in undesirably high measurement errors. Needs related to ductwork monitors vary across nuclear facilities, depending on the expected measurement location and facility layout. Two distinct frameworks for power and data transmission have been developed to accommodate indoor and outdoor monitoring points. The first is designed for readily reachable points and uses power-over-ethernet (PoE) for device power and communications. The second is designed for monitoring points to which running wired connections is not feasible. In this framework, the device is battery-powered, supports solar charging and wireless communication, and counts only periodically throughout the day. The prototype holdup monitors are collimated self-contained units combining a scintillator, photomultiplier tube (PMT) or silicon photomultiplier (SiPM), and custom control and counting electronics. Different types of scintillators may be used depending on facility sensitivity and cost requirements. Benchtop prototypes were built using sodium iodide (NaI) and plastic scintillator–based detector assemblies; these were validated with a range of radioactive sources to test the efficacy, accuracy, and detection limits of the counting electronics. The count rates detected by the electronics were compared to standard Nuclear Instrumentation Modules (NIM) bin acquisition and showed excellent agreement, within 20 counts. This paper describes the approach being pursued, discussing the efforts to design, construct, and test a prototype detector and associated counting electronics. Such a holdup monitor will aid greatly in material accountancy efforts and reduce risk to personnel.

Keywords:holdup, distributed measurement systems, radiation monitor, materials control and accounting

*goetzkc@ornl.gov

1. INTRODUCTION

Holdup monitoring is an essential part of the material accountancy necessary for any work with special nuclear material [1, 2]. Although the portion of material being produced that escapes and builds up in the ductwork is relatively small, finding the contaminated locations presents an inordinate burden to facilities: the current method requires manual measurements of hundreds of points across a given facility. Some of these points pose safety hazards to personnel because they are difficult to reach, requiring ladders. Because of the volume of measurement areas, measurement times are short, often $\leq$10 seconds, leading to large measurement errors, and measurements are only performed periodically, often on a biannual basis. As the nuclear industry continues to grow, so will the number of facilities that require holdup. Researchers at Oak Ridge National Laboratory (ORNL) are developing an inexpensive distributed holdup monitor in an effort to alleviate the burden on facilities. The holdup monitors will be ruggedized to survive exposure to the elements and will work together in concert to enable real-time, low-error measurements with automated reporting on unit health and alarm status.

2. DETECTOR CHARACTERISTICS

2.1. Base Configuration

The base configuration of all the holdup monitors is shown in Figure 1. Each detection unit will contain a scintillator, either sodium iodide (NaI) or EJ200-NF plastic; a method of reading out the scintillator, either a photomultiplier tube (PMT) or silicon photomultiplier (SiPM); collimation for background reduction; the acquisition circuitry; and water-proof aluminum housing. Aluminum is desirable because it is highly permeable to γ rays across a broad range of energies.

Each detector unit will be fitted with a light-emitting diode (LED) that may be pulsed as a “life check” on a given monitor.

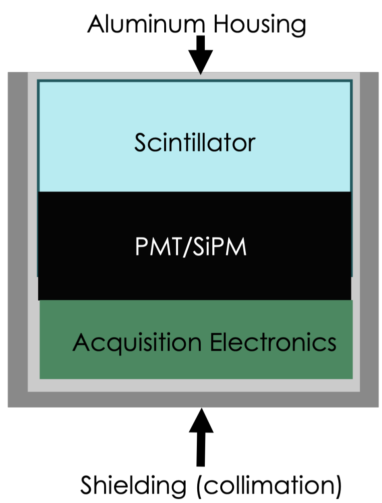

Figure 1: Base detector configuration showing a scintillator coupled to readout electronics, either a PMT or SiPM, inside of a collimator for background reduction, and acquisition electronics, all packaged within aluminum housing.

2.2. Detector Menu

A holdup monitor must be able to accommodate the needs of a range of facilities. Each individual facility is expected to have hundreds of measuring points, some indoors, some outdoors, and some in locations to

Table 1: Detector options based on location and facility requirements.

	Reachable Locations	Unreachable Locations
Scintillator	EJ200-NF (Eljen) NaI (Saint Gobain)	EJ200-NF (Eljen)
Power Schema	Power over Ethernet	Battery powered with solar panel
Communication Schema	Constant communication with central hub	Periodic communication via low power wireless signal

which running cables is very difficult. To that end, a detection "menu," shown in Table 1, was constructed. Work thus far has focused on the reachable option.

Plastic scintillators, such as EJ-200 from Eljen, are non-hygroscopic and, therefore, do not require hermetic sealing. However, some formulations of plastic scintillators are prone to "fogging" during prolonged outdoor use. Fogging is a phenomenon whereby water ingresses into the detector plastic itself after successive heating and cooling of the detector, resulting in a cloudy appearance and a marked decrease in performance [3]. Therefore, EJ200-NF is chosen for its non-fogging properties, as it is expected to increase the longevity of the end monitor. However, some facilities, or locations within facilities, will require higher-fidelity measurements. In these cases the more expensive but more than doubly sensitive NaI is recommended [4–6].

For scintillator readout, the authors expect that SiPMs will be favored over PMTs because of their smaller size and relative temperature resistance [7]. In locations that may be reached by cables, the monitors will communicate and be powered using Ethernet cables using power-over-ethernet (PoE). In locations unreachable via cables, the units will be battery powered with solar power–based energy harvesting. These detectors will communicate only periodically, via an industrial wireless process for added security. The PoE-based detectors will communicate constantly with an alarming scheme discussed below.

2.3. Prototype Detectors

To identify the optimal solution for all the facility locations and test them with the counting electronics developed as part of this project, several detector configurations are being evaluated. The three currently in-house are shown in Figure 2. These three options are composed of a 2×2" EJ200-NF plastic scintillator temporarily coupled to a Hamamatsu R6231 PMT, a 2×2" NaI permanently coupled to a PMT by Saint Gobain Crystals with model number 2M2/2-LED-X, and a 2×2" NaI permanently coupled to an array of 16 SiPMs by Saint Gobain Crystals with model number Si50.8NI50.8B75. An EJ200-NF plastic scintillator coupled to a SiPM is on order, but these have not yet been received. The NaI coupled to a PMT from Saint Gobain Crystals also includes an LED integrated into the package on the face of the PMT.

2.4. Fieldable Detector Housing

Any fieldable detector unit will require an external waterproof housing for the electronics, detector, and collimator. The first prototype of the fieldable housing is shown in Figure 3. The outer housing, shown in Figure 3b is an aluminum box with a milled viewport to a screen that will show count rate, a milled port for an Ethernet cable, and a 3D printed support for attachment to a duct. The internals of housing includes a mount for the data acquisition system, as well as a 3D printed housing for the SiPM-based 2" NaI detector from Saint Gobain and a 0.25" thick tungsten-grit and polyvinyl chloride (PVC) collimator, which is ∼80% the density of lead, leading to a ∼50% reduction in γ rays from ^{238}U.

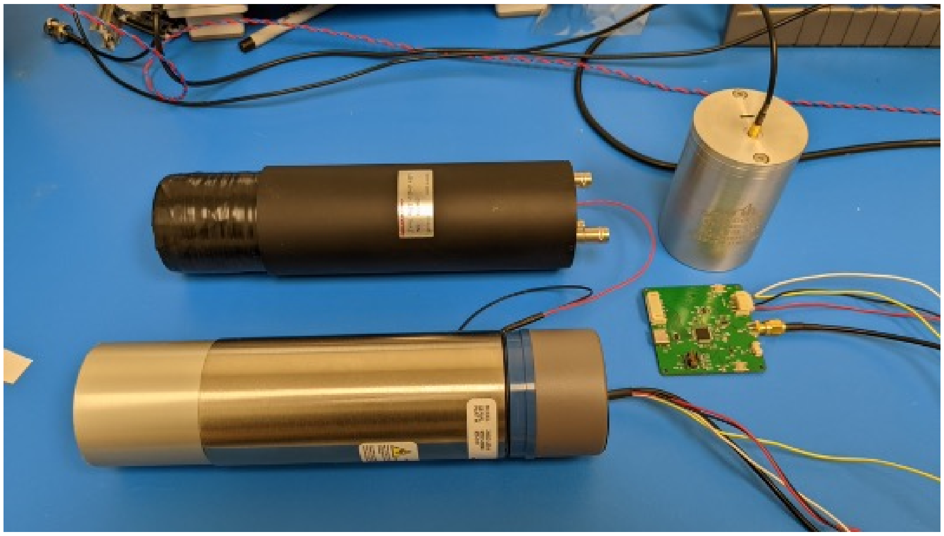

Figure 2: Three benchtop detector options currently being evaluated. The top left is a 2×2" EJ200-NF plastic scintillator temporarily coupled to a Hamamatsu R6231 PMT. Bottom left is a 2×2" NaI permanently coupled to a PMT by Saint Gobain Crystals, and top right is 2×2" NaI permanently coupled to an array of 16 SiPMs by Saint Gobain Crystals.

3. DATA ACQUISITION SYSTEM

3.1. Hardware

To support benchtop testing and a fieldable prototype, custom electronics and several printed circuit boards (PCBs) for distributed long-term monitoring of holdup have been designed. There are variants to support both PMT and SiPM detectors. The PMTs are biased with compact high-voltage (HV) power supplies using either an active voltage divider or a Cockcroft-Walton (CW) multiplier for a lower power option. The more compact and robust SiPM-based variants use a commercial off-the-shelf (COTS) solution from Saint-Gobain with integrated bias generator and temperature gain compensation. Work is ongoing to design custom electronics for future lower-cost SiPM- and plastic scintillator-based designs.

The analog, digital, and HV power supplies are regulated from a single 5 V power source. For the PoE variant, the 5 V source is derived from the provided 48 V using an IEEE 802.3af compliant DC/DC converter. The energy harvesting design integrates a 800 mA linear battery charger suitable for charging from solar cells. The battery pack will comprise single Li-ion cells assembled in parallel for the desired capacity. The required 5 V will be boost converted from the nominal 3.7 V of the battery pack. The required battery capacity and the possible observation duty cycle required for long-term monitoring is a target of future work.

Fewer signal processing electronics are required for gross counting than are required in spectroscopy applications. This is an opportunity to significantly reduce the cost and power consumption due to the supporting electronics of each unit. The PMT variants include a configurable charge-sensitive amplifier designed to operate from a single power supply with pulse shaping and using minimal components. The integrated SiPM detector from Saint Gobain includes a fixed charge-sensitive amplifier without shaping. Future work to design custom SiPM detectors will aim to reduce the cost and power consumption of the sensor itself.

The discriminator uses an analog comparator integrated into the digital electronics of the microcontroller. This approach not only reduces number of components, but it also permits a tighter integration with software. The design leverages low-cost microcontrollers for communications and control. High-performance microcontrollers are used for the PoE variant; ultra-low-power microcontrollers are used for more power-conscious and potentially wireless designs. The second prototype PCB with an ultra-low-power microcon-

(a) Internal view (b) External view

Figure 3: First prototype of fieldable housing for the detector, collimator and associated acquisition electronics. This unit is designed for the 2×2” NaI-based detector coupled to an array of SiPMs from Saint Gobain Crystals.

troller and PMT electronics is shown in Figure 4. Given the capabilities and connected nature of this sensor, we consider it an industrial internet-of-things (IIoT) device for distributed holdup monitoring.

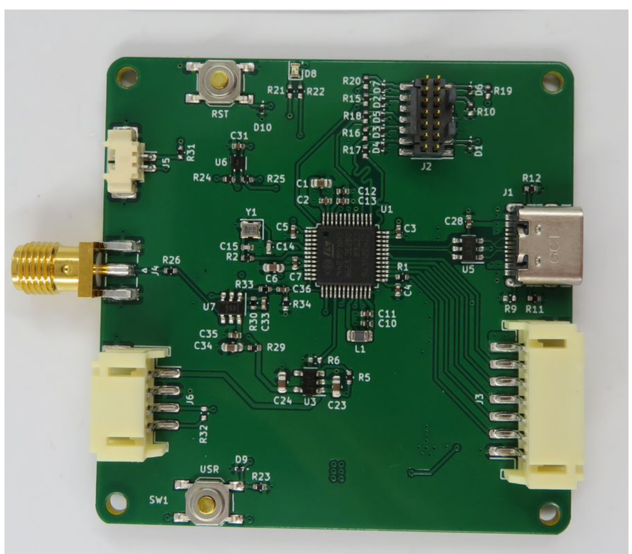

Figure 4: Second prototype PCB with ultra-low-power micro-controller and analog electronics.

3.2. Software

An embedded software development kit (SDK) has been developed that supports current and future hardware to allow custom applications to integrate a customers proprietary algorithm or to address a specific need of a facility. The aim is to provide a platform that can be deployed and updated stand alone rather than requiring additional equipment such as a co-located computer. To support this goal, the SDK has been developed based on the scalable Zephyr real-time operating system (RTOS). This SDK provides a platform with device driver abstractions and subsystems ideal for developing complex applications on resource-constrained devices.

As development of firmware for the recently manufactured hardware has just begun, development will continue as facilities weigh in with feedback about how best to accommodate their particular needs. The basic operation of the counter application is that events are triggered by the analog comparator; these are counted, and an internal timer is used to calculate the counts per second with a runtime-configurable interval. This discriminator function is implemented as a hardware-independent device driver that is compatible with all hardware support by the SDK. Software for the gain stabilization of the PMT using the embedded LED is underway while the SiPM detectors integrate automated gain stabilization. The PoE device is the current focus: counts per second and health status will be transmitted to a remote server over a secure network using TCP/IP sockets and a simple protocol. Eventually, e bidirectional communications for device control and remote maintenance will be included. The details of the communications protocol are still being examined as the needs of customers are evaluated.

4. BENCH TOP MEASUREMENTS

4.1. Validation of Counting Circuitry with NIM Electronics

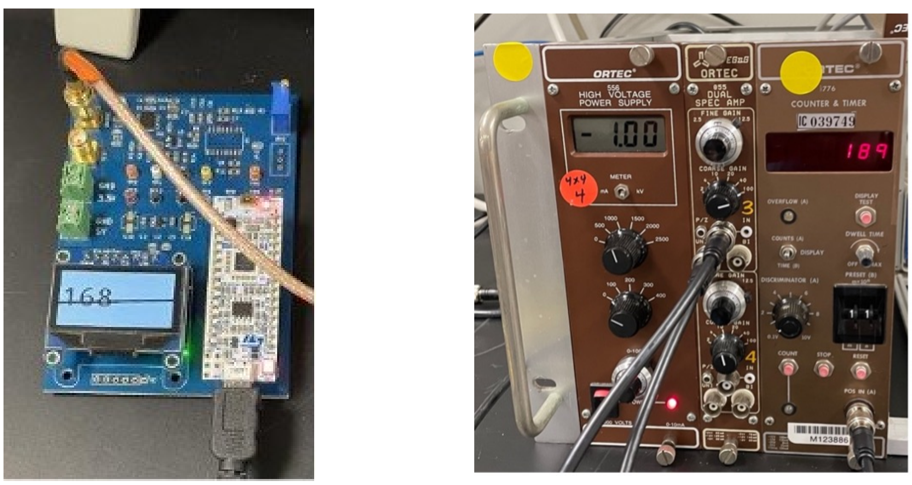

(a) Rev0 **(b) NIM**

Figure 5: The Rev0 (a) counting electronics were validated against industry standard NIM (b) electronics.

To validate the efficacy and accuracy of the counting electronics, the Rev0 counting electronics were compared to industry-standard Nuclear Instrumentation Modules (NIM) counting electronics; the results are shown in Figure 5. A 1 μC ^{137}Cs source was placed 1.9" away from the EJ200-NF/PMT detector assembly, a position chosen to maximize rate and minimize pulse pileup, as determined with an oscilloscope. The PMT was biased to a voltage of -1000 V using an Ortec 556 high-voltage power supply. The output from the PMT was sent to an Ortec 855 dual spectroscopy amplifier, serving to amplify and invert the signal from the PMT to a positive going signal. The unipolar output of the amplifier was then supplied to an Ortec 776 counter and timer module for event counting. The output of the PMT was alternatively linked to the rev0 counting electronics, showing count rates within $\sim$20 cps of each other, a slight discrepancy that can be explained by slight movements in detector position due to cable movements in the change over between the electronics.

Table 2: Sources measured for efficiency calculation and their associated γ-ray energies.

Source	γ-ray energy (keV)
^{241}Am	56
^{133}Ba	82
^{137}Cs	662
^{60}Co	1172,1332

4.2. Energy-Dependent Efficiency

The desired detection range is between 100 keV and 2 MeV. To test detection efficiency over this range, a selection of sources representing low-, mid-, and high-energy γ rays were measured at a distance of 1.9" from the front face of the scintillator for 10 minutes each, using the plastic and NaI PMT-coupled detectors. Room background was also measured for 10 minutes. The sources and their pertinent γ-ray energies are shown in Table 2. Source activity (R) was calculated using the assay date and activity labeled on the source using Equation 1:

$$R = R_o e^{-\frac{t}{\lambda}} \quad (1)$$

where R_o is the activity on the assay date, t is the time since the assay, and λ is the half-life of the isotope.

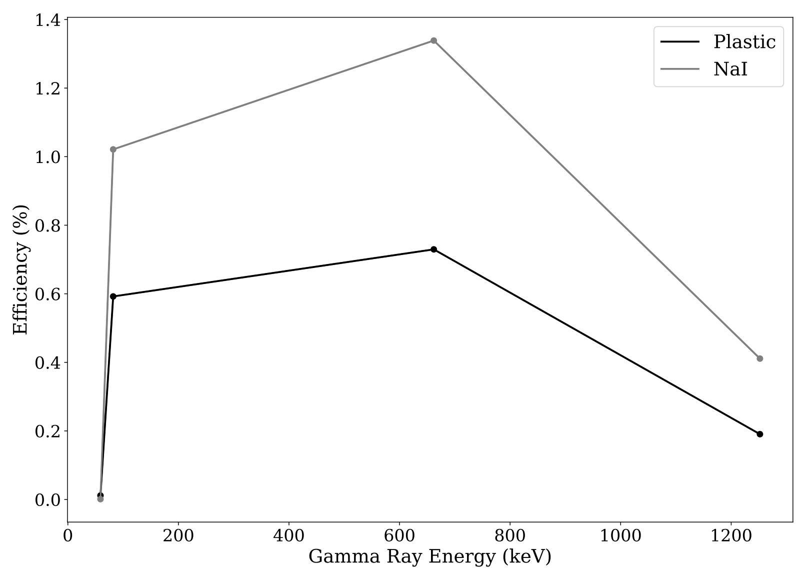

Figure 6: Efficiency curves for the 2" NaI and EJ200-NF plastic scintillator detectors.

As the counting electronics report counts per second (cps) once every second, these values were recorded and fit with a normal distribution, given by Equation 2, to find an average cps over the counting period.

$$f(x) = \frac{1}{\sigma_n \sqrt{2\pi}} e^{-\frac{1}{2}\left(\frac{x - x_o}{\sigma_n}\right)^2} \quad (2)$$

Here, σ_n is the standard deviation, and x_o is the mean.

The error σ in the count rate then becomes $\sigma = \frac{\sigma_n}{\sqrt{N}}$, where N is the number of seconds in the measurement period. The efficiency E for each source is given by Equation 3.

$$E = \frac{x_0}{R \cdot I_\gamma} \tag{3}$$

In Equation 3, I_γ is the absolute intensity of the γ ray. The resulting efficiency curve for both plastic and NaI scintillators coupled to PMTs is shown in Figure 6.

The swift drop in efficiency for the lowest energy γ ray, 56 keV, is due to threshold effects in the counting electronics. Threshold has been set to be above background fluctuations to prevent erroneous count rates but is still minimized to maintain a low detection threshold. A 56 keV γ ray is well below the minimum desired threshold of 100 keV. In fact, the efficiency curve shows that 100 keV γ rays are in a highly-sensitive portion of the detection range, which is desirable given that most of the γ rays emitted by the relevant isotopes of uranium and plutonium are in the 100 keV range.

4.3. Maximum and Minimum Count Rates

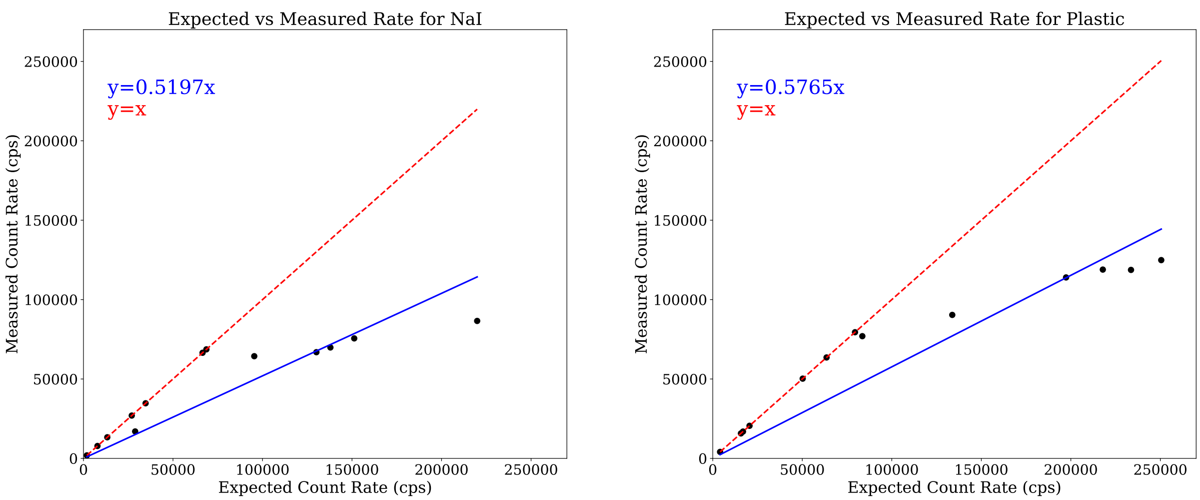

(a) **(b)**

Figure 7: Expected versus measured count rates for NaI and plastic PMT-coupled detectors. The red dotted line represents y = x; the blue line is the line of best fit through the origin for data.

Linearity in count rate was measured by placing a range of sources on the scintillator face for both the plastic and NaI PMT-coupled detectors. The sources were measured individually to provide an expected count rate as they sum together; they were then measured in combination, providing raised count rates. Each measurement was two minutes in duration, with the reported cps values fit with a normal distribution to provide an average count rate and measurement error. The expected average count rates were then plotted against the measured average count rates (Figure 7) along with a $y = x$ (dotted red) line for reference and a line of best fit (blue) through the origin.

In both the NaI and plastic-based detectors, the count rate becomes highly nonlinear at around 100,000 cps. This divergence in both detectors at the same point suggests that the non-linearity rests within the counting electronics. Pulse pileup in the scintillators themselves is unlikely to be the cause, as the primary decay times of NaI and EJ200-NF are vastly different—250 ns and 16 ns, respectively. However, the decay time of the pulse of the detector electronics is configured to be on the order of several microseconds. The reason for the count rate nonlinearity is currently under investigation. The latest revision of the board includes additional pulse shaping that has yet to be tested. The digital electronics starting at the comparator will also be tested.

In any case, 100,000 cps is well above the threshold at which a detector unit should alarm; therefore, this nonlinearity in count rate is not of great concern.

4.4. Simulated Holdup

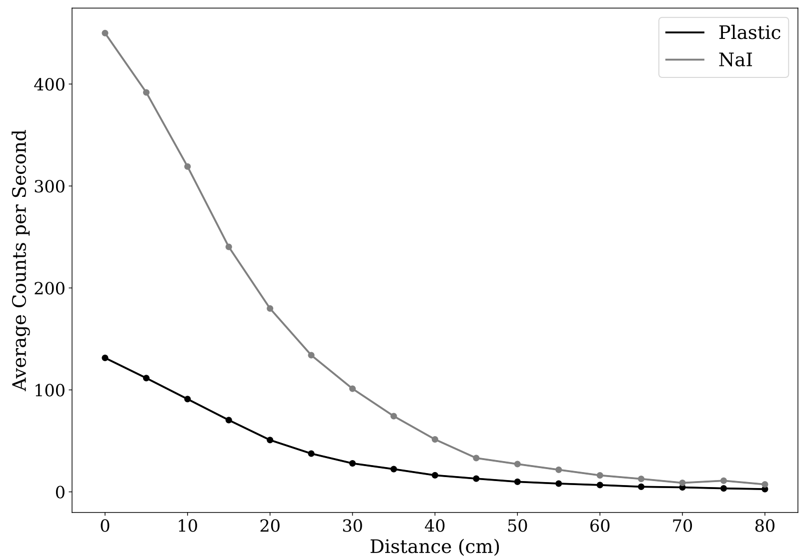

Figure 8: Simulated holdup measurement using NaI and plastic-based detectors. Detectors were moved closer to the source in 5 cm steps, collecting for two minutes at each step.

The final benchtop test performed to date is simulated holdup. A 200 g sample of 4.46% enriched U_3O_8 was placed inside of a 0.26 cm thick 30 cm inner diameter stainless-steel pipe with a meter stick on the top of the pipe marking distance from the source. The source was positioned so that it was roughly in the centerline of the pipe. The source was collected for two minutes; collections were done at varying distances along the pipe with both the NaI and plastic scintillator detectors coupled to PMTs. A normal distribution was fit to the count rates, producing an average count rate for each measurement position and background subtracted; the results are shown in Figure 8.

NaI is more sensitive, by more than a factor of two, than the plastic detector, as is expected. With the assumption of a 2σ detection limit above background, this means that the NaI-based detector alarmed at $\sim$65 cm away from the source, whereas the plastic-based detector alarmed at $\sim$50 cm.

5. ALARMING SCHEMA

Facility backgrounds are expected to fluctuate based on location, time, operational status of the facility, and so on. If left unaccounted for, these fluctuations could lead to many false positive and negative alarms.

One possibility to deal with fluctuating background levels is to strategically place extra detectors measuring only background around the facility and combine those with extra collimation on each detector unit. However, this will incur further cost to the facility in the form of additional, and more expensive, detectors—as well as their associated maintenance costs; therefore, this approach less desirable.

A second possibility being explored is to treat every detector unit as both background and detector. As each facility is expected to have hundreds of monitoring points, detectors may be divided up into groupings of similar background levels and still be numerous enough to provide statistically significant results for backgrounds and alarms.

To explore this schema, the authors have developed a software simulation tool which a group of N detectors are simulated with some number alarming and some number broken. Here, detectors are randomly assigned a count rate for a given counting period within a normal distribution representing a background. Another subset is likewise randomly assigned a count rate within a normal distribution around some elevated number of counts; these are the alarming detectors. Finally, another subset is assigned a low count rate, again randomly chosen from a normal distribution. The entire detector set, including broken and alarming detectors, is then fit with its own normal distribution. Detectors that are some number of σ above and below average are considered to be alarming or broken, respectively, for that given count period. An alarm becomes a true alarm after a detector has been alarming consistently for some number of counting periods.

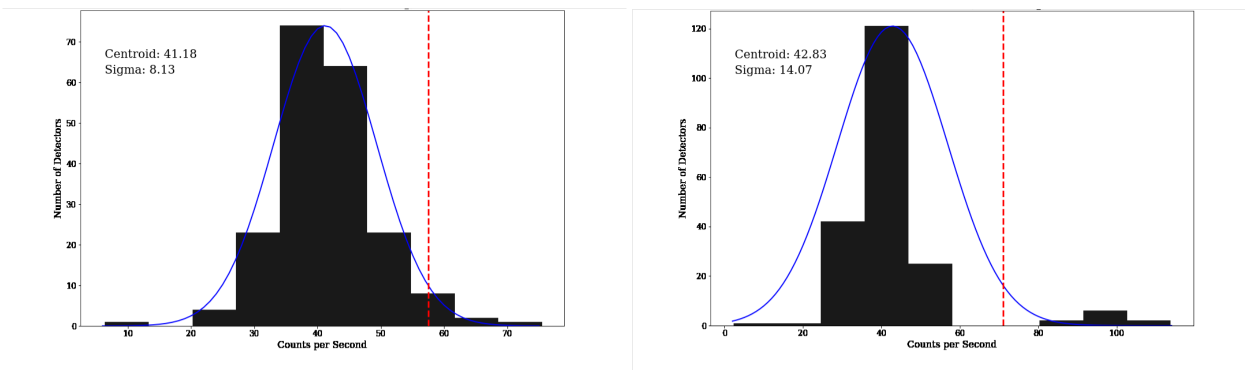

(a) **(b)**

Figure 9: A simulation of a grouping of 200 detectors, 10 of which are alarming and 1 of which is broken.

Results for a grouping of 200 detectors, 10 of which are alarming and 1 of which is broken, are shown in Figure 9. The dotted red line indicates a 2σ limit above which a detector is considered to be "alarming" for this counting period. The detectors measuring background are seeing a background rate of 40 cps with a $\sigma = 6$ cps spread, a number arrived at through background measurements in the laboratory. In Figure 9a, the 10 alarming detectors are seeing a 60 cps rate with a $\sigma = 6$ cps spread. The 10 alarming detectors in Figure 9b are seeing a 100 cps rate with a $\sigma = 6$ cps spread. In both cases, the single broken detector is seeing 5 cps rate with a $\sigma = 5$ cps spread. The entire detector grouping is fit with a normal distribution, which should report back the background rate. The grouping with 10 detectors seeing an "alarm" at 20 counts above background reports a 41 cps centroid and a 8 cps spread; the grouping with 10 detectors seeing an "alarm" at 60 counts above background reports a 43 cps centroid and a 14 cps spread. In both cases, the background rate is well reproduced. The +20 cps alarm grouping is not entirely identified for this counting period, with two false alarms, and the +60 cps alarm grouping is entirely identified with the 2σ detection limit.

The advantage of this method is that background levels may fluctuate between counting periods with no effect on the false positive or negative alarm rate, and there are no increases to facilities costs in the form of additional detectors. A few assumptions were made, however. The first is that the majority of the detectors are both functional and not alarming during any given measurement period. The second is that all detectors are recording similar background rates and those rates due not fluctuate wildly during the counting period.

The alarming schema's sensitivity to factors such as the number of detectors in the group, statistical spread in the rate background, and the number of detectors alarming or broken during each counting period are still being explored.

6. CONCLUSIONS

Several benchtop prototypes of a holdup monitor and associated counting electronics were fabricated and tested. The results show that these prototypes perform well under laboratory conditions for the desired γ-ray energy range and count rates expected at the relevant facilities. Further work is underway to perform environment resistance testing with a first prototype of a ruggedized collimated detector unit capable of field measurements in hand.

An alarming schema that takes advantage of the distributed network of sensors is under development. The schema allows for variation in background rates across the detector network and automatically identifies alarming and broken detectors. Its limitations and full implementation are still under development.

Researchers have developed two early prototype PCBs to test the initial electronics design. Lessons learned from testing these designs have already been incorporated into the schematics in the next design to be manufactured this year. Electronics supply chain issues limited the design of these early prototypes. As the supply chain issues have begun to subside, many of the parts required for more advanced and robust designs are now procurable. Developing the firmware and will continue in parallel with new hardware to support our current and future low-cost, distributed detector systems.

ACKNOWLEDGMENTS

The authors would like to thank Lorenzo Fabris for his guidance and Brandon Longmire for designing, milling, and printing the fieldable detector housing. This work was funded under the Department of Energy Nuclear Engineering Office as part of the MPACT program.

REFERENCES

[1] KKS Pillay. Holdup-related issues in safeguarding of nuclear materials. *JNMM*, 26(4):18–21, 1988.

[2] J Beckers, P Jaunet, M Boella, W Koehne, B Burrows, C Koutsoyannapoulos, A Colin, J Pattern, M Crousilles, E Pujol, et al. Control of nuclear material hold-up: The key factors for design and operation of mox fuel fabrication plants in europe. Technical report, 2001.

[3] Michael J Lance, Natalia P Zaitseva, Stephen A Payne, Richard T Kouzes, Nicholas R Myllenbeck, and Alan Janos. Nature of moisture-induced fogging defects in scintillator plastic. *Nuclear Instruments and Methods in Physics Research Section A: Accelerators, Spectrometers, Detectors and Associated Equipment*, 954:161806, 2020.

[4] Saint Gobain Crystals. Nai(tl) scintillation crystals.

[5] Eljen Technology. Non-fogging plastic scintillators.

[6] Matthieu Hamel, Pawel Sibczynski, Pauline Blanc, Joanna Iwanowska, Frédérick Carrel, Agnieszka Syntfeld-Każuch, and Stéphane Normand. A fluorocarbon plastic scintillator for neutron detection: Proof of concept. *Nuclear Instruments and Methods in Physics Research Section A: Accelerators, Spectrometers, Detectors and Associated Equipment*, 768:26–31, 2014.

[7] M Petasecca, B Alpat, G Ambrosi, P Azzarello, R Battiston, M Ionica, A Papi, GU Pignatel, and S Haino. Thermal and electrical characterization of silicon photomultiplier. *IEEE Transactions on Nuclear Science*, 55(3):1686–1690, 2008.